Shape of the hydrogen adsorption regions of MOF-5 and its impact on the hydrogen storage capacity

I. Cabria,[1] M. J. López,[1] and J. A. Alonso[1,2]
[1]*Departamento de Física Teórica, Atómica y Óptica, Universidad de Valladolid, 47005 Valladolid, Spain*
[2]*Donostia International Physics Center (DIPC), 20018 San Sebastián, Spain*
(Received 18 July 2008; revised manuscript received 11 October 2008; published 24 November 2008)

The adsorption of molecular hydrogen on a metal-organic framework (MOF) material, MOF-5, has been studied using the density-functional formalism. The calculated potential-energy surface shows that there are two main adsorption regions: both near the OZn_4 oxide cores at the vertices of the cubic skeleton of MOF-5. The adsorption energies in those regions are between 100 and 130 meV/molecule. Those adsorption regions have the shape of long, wide, and deep connected trenches and passage of the molecule between regions needs to surpass small barriers of 30–50 meV. The shape of these regions, and not only the presence of metal atoms, explains the large storage capacity measured for MOF-5. The elongated shape explains why some authors have previously identified only one type of adsorption site, associated to the Zn oxide core, and others identified two or three sites. One should consider adsorption regions rather than adsorption sites. A third region of adsorption is near the benzenic rings of the MOF-5. We have also analyzed the possibility of dissociative chemisorption. The chemisorption energy with respect to two separated H atoms is 1.33 eV/H atom; but, since dissociating the free molecule costs 4.75 eV, the physisorbed H_2 molecule is more stable than the dissociated chemisorbed state by about 2 eV. Dissociation of the adsorbed molecule costs less energy, but the dissociation barrier is still high.

DOI: 10.1103/PhysRevB.78.205432 PACS number(s): 68.43.−h, 84.60.−h, 61.43.Gt, 73.22.−f

I. INTRODUCTION

The Department of Energy (DOE) established hydrogen storage targets for onboard automotive applications.[1,2] The targets for 2010 are at least 6% of the storage system weight and 0.045 kg of hydrogen/l. These targets would allow using hydrogen as a fuel in cars with an autonomy range similar to the present gasoline cars. The targets for 2015 are more strict: 9 wt % and 0.081 kg H_2/l. In the search for promising hydrogen storage materials, several paths have been followed. Carbon nanotubes (CNTs) were considered a promising candidate ten years ago because of their large surface area and light weight. Nowadays, after many experimental and theoretical studies, the general consensus[3,4] is that undoped CNTs adsorb little hydrogen (less than 1 wt % at room temperature and moderate pressures).

In 1999 Hailian *et al.*[5] synthesized a porous metal-organic framework (MOF) material, which remained crystalline and stable in the absence of guest molecules and when heated up to 573 K, and measured its gas storage capacity. They called this new material as MOF-5. Previous open MOFs were not stable and collapsed. MOF-5, later also called isoreticular MOF (IRMOF-1), is a material formed by OZn_4 tetrahedra linked by 1,4-benzene-dicarboxylate (BDC) groups (O_2C-C_6H_4-CO_2), briefly BDC groups, forming a network of empty cubes, as can be seen in Fig. 1. The OZn_4 tetrahedra are at the corners of the cubes. A few years later, the same group proposed that MOF-5 was a promising candidate for on-board automotive hydrogen storage[6] and this was confirmed by other experimental reports. Rowsell *et al.*[7] measured a storage capacity of 1.32 wt % at 1 atm (0.101 MPa) and 77 K and Wong-Foi *et al.*[8] reported storage capacities of 5.2 wt % and 0.030 kg/l at 5 MPa and 77 K. Panella *et al.*[9] obtained 4.7 wt % at 5 MPa and 77 K (and an extrapolated saturation value of 5.1 wt %) and 0.28 wt % at 6.5 MPa and 300 K. The stored hydrogen is in a physisorption state. Using inelastic neutron scattering, Rosi *et al.*[6] observed two different hydrogen adsorption sites and associated one with Zn and the other with the BDC linker.

MOF-5 was the first tested member of another family of highly porous crystalline materials, MOFs. These materials can be produced at low cost. They hold the record in specific surface area (SSA) (Ref. 10): the estimated SSA of MOF-177 is 4500 m^2/g. MOFs have applications in catalysis, in the storage of gases, hydrogen, and methane among others, and in the separation of gases. Because of the structural richness of MOFs, the number of newly investigated materials of this family is increasing. Besides, the structure and pore size can be engineered and controlled by using appropriate metal atoms and organic linker molecules, which, in turn, allow us to tune the gas storage capacity of this family of materials. Adsorption of H_2 molecules on the MOFs can occur on different sites: on the organic groups as well as near the metal cores (BDC groups and OZn_4 tetrahedra, respectively, in MOF-5). This helps to understand why the MOFs may have large storage capacities, of the same order of magnitude, or perhaps larger than those of activated carbons and carbide-derived carbons.

Some theoretical studies of the hydrogen adsorption on MOF-5 (Refs. 11–14) found that the physisorption energies near the OZn_4 tetrahedra are larger than in other parts of the structure of the MOF-5. However, Mulder *et al.*[15] predicted similar physisorption energies on the BDC linkers and near the metal cores. Although it is believed that the adsorption mechanism of hydrogen on MOFs is physisorption, the dissociative chemisorption and the physisorption-chemisorption barriers have not been studied and it should be useful to confirm this view.

In this paper we present density-functional calculations of the adsorption of H_2 on MOF-5. The details of the computa-

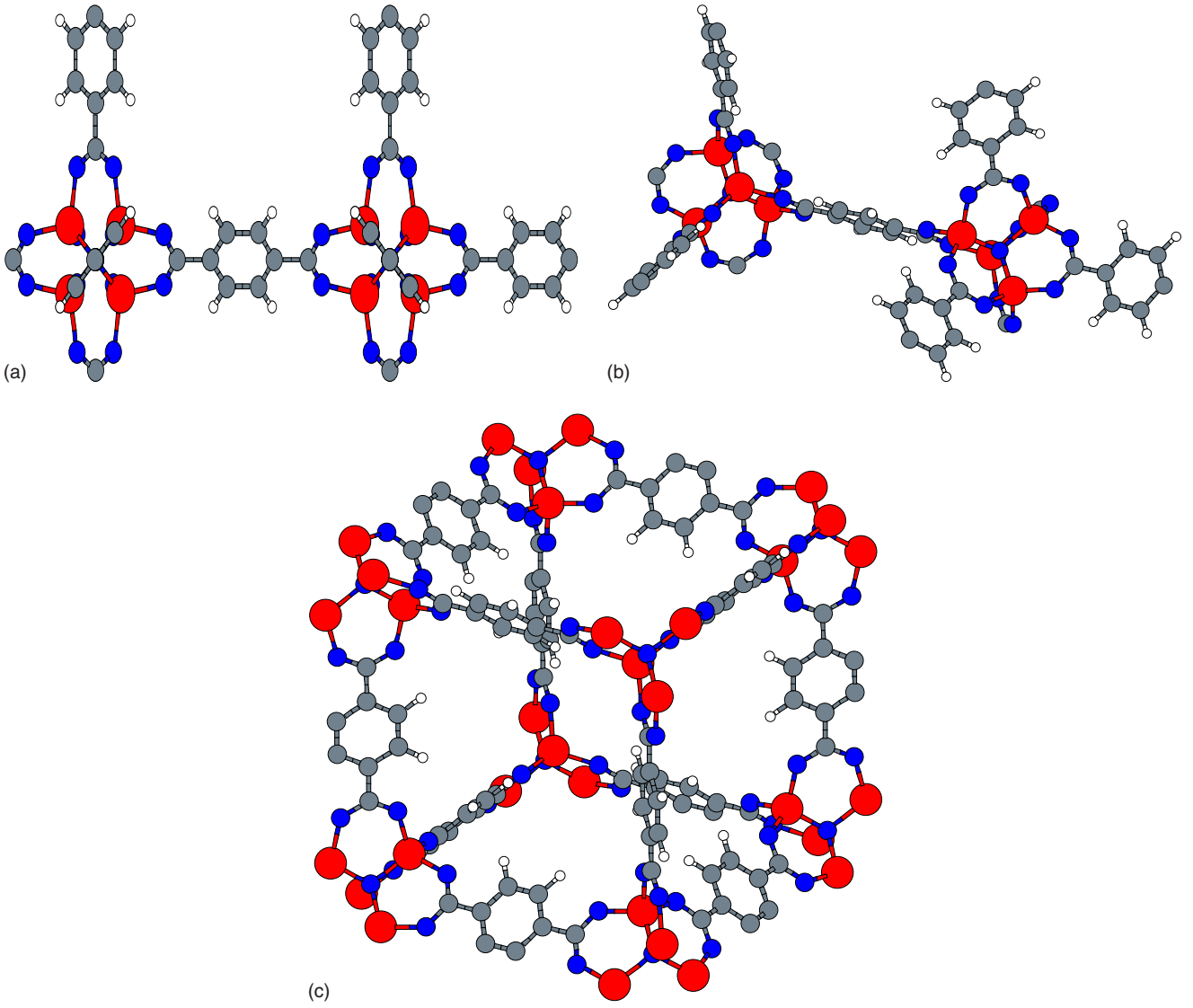

FIG. 1. (Color online) Optimized geometry of MOF-5: two views of the unit cell with 106 atoms used in the calculations (top panels) and MOF-5 cube (bottom panel). Colors: blue (O atoms), red (Zn atoms), gray (C atoms), and white (H atoms). The structure is formed by OZn_4 tetrahedra at the corners linked by BDC groups.

tional method are described in Sec. II. The adsorption of molecular hydrogen is studied in Sec. III and the favorable adsorption regions are identified and discussed by analyzing the potential-energy surface. We have also studied the dissociative chemisorption and the barriers for dissociative chemisorption in Sec. IV. Section V presents the conclusions of this work.

II. COMPUTATIONAL METHOD

We have performed density-functional calculations with the local-density approximation (LDA) (Ref. 16) for exchange and correlation effects using the DACAPO code.[17] A basis of plane waves to expand the wave functions and ultrasoft pseudopotentials are employed in the code. In the calculations for the clean MOF-5 we used a [111] Monkhorst-Pack κ-point set, a wave-function cutoff of 500 eV, and a cutoff of 1000 eV for the density. This κ-point set and cutoffs were chosen after several tests to guarantee a precision of 0.01 eV in the cohesive energy per atom and a smooth energy curve as a function of the lattice parameter a. However, in the calculations for the adsorption of H_2 on MOF-5, we used 300 and 500 eV for the wave-function and density cutoffs, respectively. These calculations consume much less time and memory resources. The tests indicate that the largest difference between the H_2 adsorption energies obtained with these and with the higher cutoffs (500 eV for wave functions and 1000 eV for densities) is only 5 meV.

The unit cell of the MOF-5 used in the present calculations is the smallest periodic cell: $[OZn_4(BDC)_3]_2$, with 106 atoms. This unit cell is periodically repeated in a fcc lattice of parameter a. The optimized unit cell is plotted in Fig. 1. Optimization of the a parameter and the coordinates of all the 106 atoms of the unit cell yielded $a=25.650\pm0.005$ Å. In Table I we compare the results of the present optimization of the MOF-5 structure with experiment and with previous

TABLE I. Geometrical parameters (distances and angles) of MOF-5 (see Fig. 3). Lengths are in Å and angles in degrees.

Parameter	Expt.[a]	This work	Samanta *et al.*[b]
	Distances		
a	25.669 ± 0.001	25.650	25.637
Zn-Zn	3.16 ± 0.01	3.14	3.14
Zn-O tetrahedron	1.91 ± 0.01	1.92	1.92
Zn-O BDC	1.91 ± 0.01	1.91	1.92
O-C	1.30 ± 0.01	1.27	1.27
	Angles		
O-C-O	125.0 ± 0.1	126.1	125.8
O-C-C	117.5 ± 0.1	116.9	117.0
Zn-O-C	130.4 ± 0.1	130.0	130.5
Zn-Zn-Zn	60.0 ± 0.1	60.0	60.0

[a]Reference 5.
[b]Reference 14.

LDA calculations by Samanta *et al.*,[14] and we obtain very good agreement with both. The density of electronic states (DOS) of this material is plotted in Fig. 2. The shape and peak positions of the DOS are very similar to those calculated by Samanta *et al.*[14] The band gap is about 2.5 eV, similar to the value of 2.7 eV obtained by Samanta *et al.*[14] and smaller than the value of 3.5 eV observed in spectroscopy experiments.[18] The underestimation of the band gap is common in LDA calculations.

III. HYDROGEN PHYSISORPTION

The adsorption energies E_b of molecular hydrogen on MOF-5 have been calculated as

$$E_b = E(\text{MOF-5}) + E(\text{H}_2) - E(\text{H}_2 - \text{MOF-5}) \quad (1)$$

obtained from the calculated energies of the clean MOF-5, the free H_2 molecule, and the MOF-5 with the adsorbed molecule. The porous structure of MOF-5 provides different adsorption sites. Our extensive calculations have revealed three main regions for hydrogen adsorption. The first two regions, which we call A and B regions, are near the metal oxide core: the OZn_4 tetrahedra shown in Fig. 1. Region A is in the cuplike volume formed by the planes of three adjacent O_{core}-Zn_A-O_A-C-O_B-Zn_B hexagons joining at a common O_{core} atom. Those hexagons and region A can be seen in the upper left panel of Fig. 3 and O_{core} is the oxygen atom at the center of an OZn_4 tetrahedron. Region B is a more open region in which the H_2 molecule is in front of a triangle formed by oxygen atoms, for instance, the triangle O_A-O_C-O_D in the upper right panel of Fig. 3. Each of those three oxygen atoms is part of a different O_{core}-Zn-O-C-O-Zn hexagon and those three hexagons share a common Zn-O side, for instance, the Zn_A-O_{core} side in the upper right panel of Fig. 3. Adsorption region C is near the benzene hexagons of the BDC linker (see lower panel of Fig. 3). Taking into account the symmetry of the structure of MOF-5, there are eight octants around an OZn_4 tetrahedron; four equivalent octants contain regions of type A and the other four octants contain regions of type B.

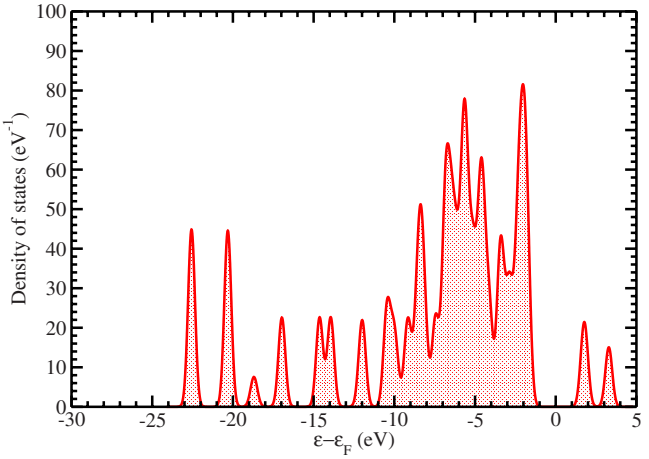

FIG. 2. (Color online) Calculated density of electronic states of MOF-5.

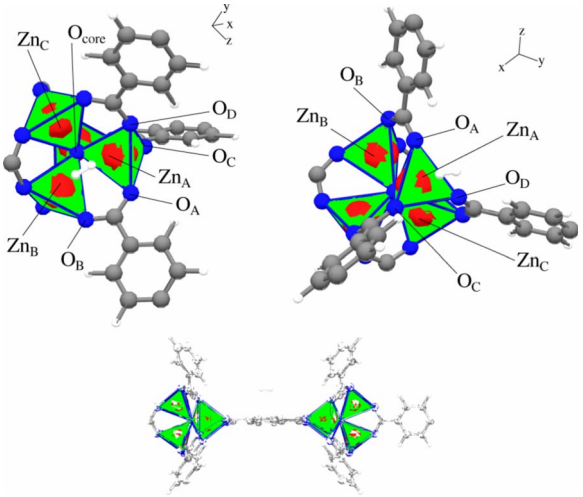

FIG. 3. (Color online) Adsorption regions of H_2 on MOF-5. Upper left: H_2 in region A (octant $x<0$, $y>0$, and $z>0$), a cuplike volume formed by three O_{core}-Zn_A-O_A-C-O_B-Zn_B hexagons sharing a O_{core} atom. Upper right: adsorption on region B (octant $x>0$, $y>0$, and $z>0$), an open region near a triangle of oxygen atoms (O_A, O_C, and O_D). Bottom: H_2 on the benzene hexagon of the BDC linker. The Cartesian axes centered on the core oxygen O_{core} are also plotted.

The largest physisorption energies occur in region A near the metal oxide core, in agreement with previous calculations.[11–14] Near the benzene hexagon of the BDC linker, region C, the adsorption energies are smaller. In region B the adsorption energies are intermediate between those in regions A and C. We show in Fig. 4 the interaction potential between the H_2 and the MOF-5 for two particular adsorption sites. One of the sites is in region A near the O_{core}-Zn_A-O_A-C-O_B-Zn_B hexagon (see upper left panel of Fig. 3) called here core hexagon and the other site is in region C on top of the benzene hexagon. These two interaction potentials are compared in Fig. 4 with the interaction

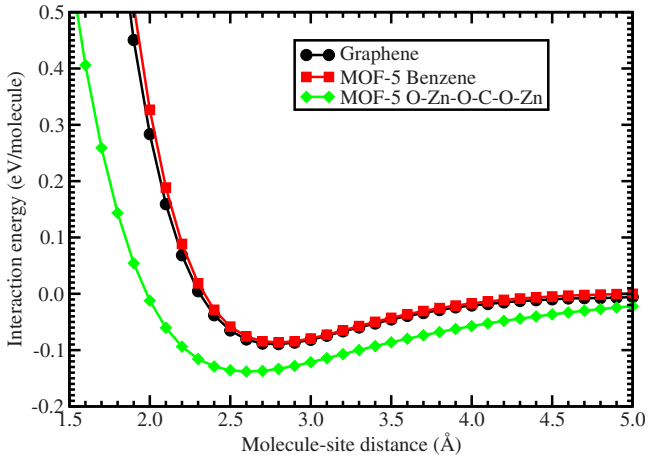

FIG. 4. (Color online) Interaction potential energy (in eV/molecule) of a hydrogen molecule adsorbed on the O_{core}-Zn_A-O_A-C-O_B-Zn_B hexagon and adsorbed on the benzene hexagon of the BDC linker of MOF-5 compared to the potential for adsorption on a graphene layer. The molecular axis is perpendicular to the plane of the hexagons.

potential for the molecule on top of a carbon hexagon of a graphene layer; a case that we have studied previously.[19] To facilitate the comparison, the molecular axis is in the three cases perpendicular to the underlying hexagon plane, and the interaction potential is plotted as a function of the distance to that plane. The depth of the potential for adsorption on the O_{core}-Zn_A-O_A-C-O_B-Zn_B hexagon (140 meV/molecule) is substantially larger than the depth of the other two potentials (90 meV/molecule). Samanta *et al.*[14] calculated a depth of 86 meV/molecule on top the benzene plane with the molecule perpendicular to the plane. We notice that the shape and depth of the interaction potential with the graphene layer and with the benzene hexagon of MOF-5 are almost identical.

The search for adsorption sites revealed that the main adsorption regions are located near the OZn_4 cores, in regions A and B described above. These regions are centered on the planes: $x=\pm y$, $y=\pm z$, and $x=\pm z$. To illustrate the trends in adsorption we plot the potential-energy surface (PES) on one of those planes with a fixed orientation of the molecular axis (we have calculated the physisorption energies for different orientations of the molecular axis, finding that there is a difference of at most 30 meV/molecule between different orientations at the same sites). Due to the symmetry of the MOF-5, the PES on many of the above planes are identical and a plane along two octants containing regions A and B is just enough to represent all the octants. We have chosen the plane $x=y$ and the octants $x>0$, $y>0$, and $z<0$, and $x>0$, $y>0$, and $z>0$, which pass through regions A and B, respectively. To represent the results, we take as reference the axes plotted in the upper panel of Fig. 3 and we have used a grid with a minimal separation of 0.25 Å between the grid points. The molecular axis is oriented in all cases pointing to the center of the oxide core atom O_{core}. The PES corresponding to the plane $x=y$ on these two octants is plotted in Fig. 5.

There are two main physisorption regions: A in the octants $z<0$ and B in the octants $z>0$, both indicated in blue color in Fig. 5. Region A is a long trench of about 100 meV/molecule deep, along the borders of the atoms in that octant. An energy minimum of the PES (in dark blue) appears well localized in the trench. This energy minimum with a depth of 130 meV/molecule is centered approximately on the point $(1.8,1.8,-1.8)$ Å, in the diagonal of this octant. That point is at equal distances of 2.6 Å from the three neighbor O-Zn-O-C-O-Zn hexagons. The areas of more attractive potential energy in the octant $z>0$ are located in region B (indicated in blue color) near the O_A-O_C-O_D plane (see upper right panel of Fig. 3). This region of high adsorption energy also has the shape of a long trench parallel to the Zn_A-O_A bond. The depth of the trench is about 100 meV/molecule.

The trenches or regions A and B are flanked on one side by repulsive potential regions looking like "mountains," representing the repulsive effect when the molecule approaches too closely to the atoms of the O-Zn-O-C-O-Zn hexagons. On the other side they are flanked by a vast flat region of almost zero interaction energy, representing the empty space of MOF-5 in that plane. Interestingly, regions A and B are interconnected, but there is a small barrier of about 30–50 meV/molecule to pass from region B to region A. Finally, region C—not plotted in Fig. 5—corresponds to adsorption on the benzene hexagon of the BDC linker. The binding energy is about 90 meV/molecule.

Both regions A and B are near the core oxide, but region A shows larger physisorption energies. Our interpretation is that the cuplike region A surrounded by three O_{core}-Zn-O-C-O-Zn hexagons provides a porelike environment where the hydrogen molecule is interacting with a larger effective surface compared to region B. Some authors have suggested that the proximity to the Zn atoms of MOF-5 is the reason of the larger physisorption energies near the oxide cores. However, as can be seen in Fig. 5, only a small volume of region B is near a Zn_A atom and the physisorption energies in that volume are similar to or smaller than the energies of many parts of regions A and B that are not in direct contact with any Zn atom. Therefore, it appears that the key for the preference for region A is not only the proximity to the transition metals of MOF-5 as many authors suggested, but also the structure or shape of the atomic environment. This implies that the presence of transition-metal atoms is not the only reason of the large physisorption energies and storage capacities of MOF-5 and other MOFs but also the shape of the physisorption regions or equivalently the structure of the atomic environment.

Adsorption on regions A and B (with adsorption energies around 130 and 100 meV/molecule, respectively) is more favorable than adsorption on the benzene ring of the BDC linker (adsorption energies between 80 and 90 meV/molecule). This is in agreement with previous density-functional theory (DFT) (Refs. 12–14) and second-order Möller-Plesset (MP2) (Refs. 11, 20, and 21) calculations, which also showed that the H_2 adsorption energies near the OZn_4 tetrahedra are larger than near the BDC linkers. In their LDA calculations Samanta *et al.*[14] obtained adsorption energies ranging between 106 and 160 meV/molecule on sites near the Zn clusters and energies of 69 and 86 meV/molecule for adsorption on the benzene molecule of the BDC linker with the molecule parallel and perpendicular, respectively, to

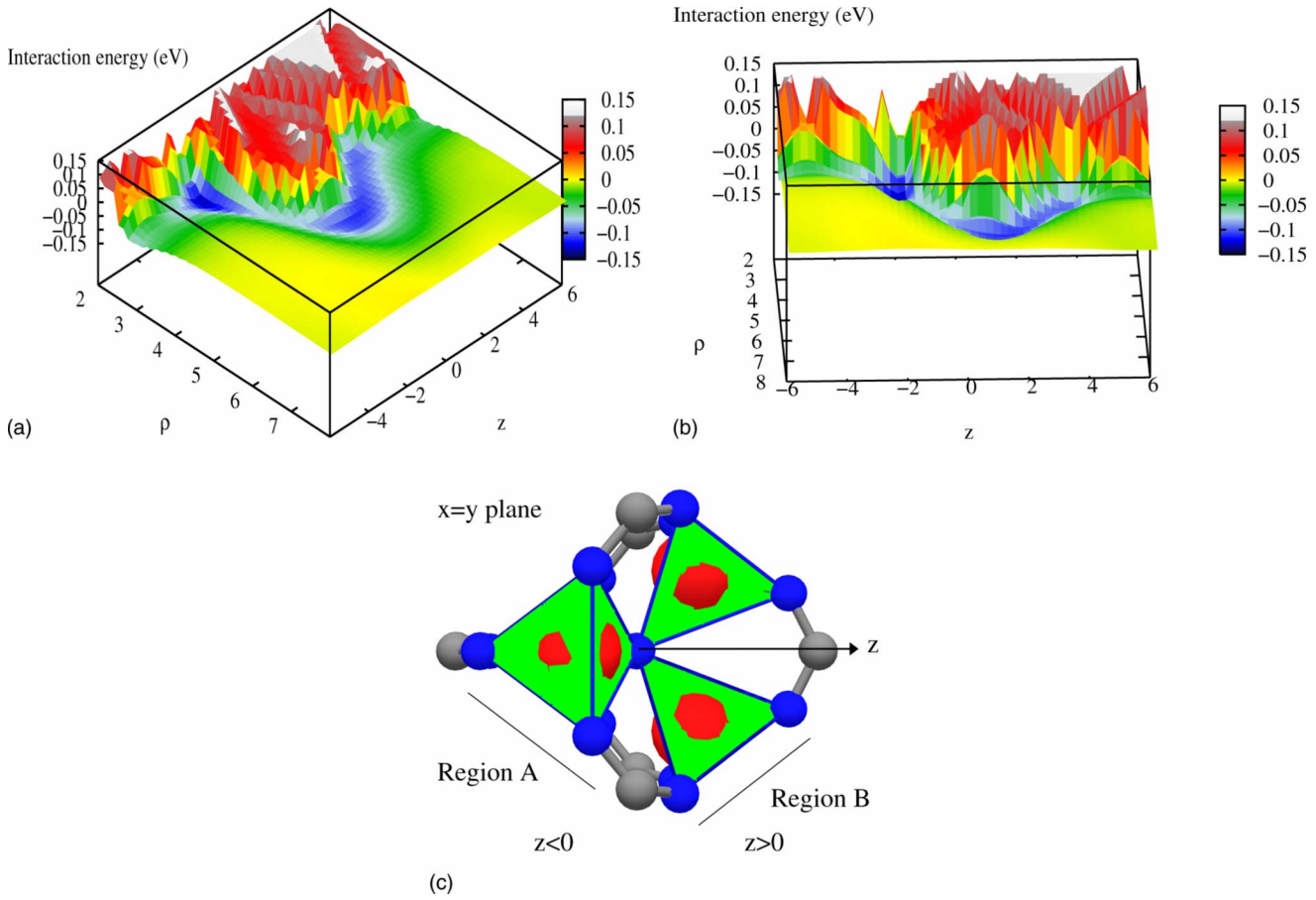

FIG. 5. (Color online) Two views of the PES of a hydrogen molecule interacting with MOF-5 on the plane $x=y$ in the octants $x>0$, $y>0$, $z<0$ and $x>0$, $y>0$, and $z>0$. Coordinate ρ is the cylindrical radial distance to the z axis. The molecular axis is in all cases oriented toward the center of the metal oxide core, the oxygen atom O_{core}. Units of the interaction energy are eV/molecule. Deep trenches of favorable adsorption are flanked by repulsive mountainlike regions on one side and by flat regions on the other. The bottom panel shows the location of regions A and B near the oxide core of MOF-5 in the $x=y$ plane.

the benzene plane. LDA calculations by Yildirim and Hartman[12] also yielded energies between 108 and 160 meV/molecule near the Zn cluster for the perpendicular orientation and between 56 and 133 meV/molecule for the parallel orientation. For adsorption on the benzene plane, they found 92 and 106 meV/molecule for the parallel and perpendicular orientations, respectively. Sagara *et al.*[11] performed MP2 calculations of the interaction of H_2 with a free benzene molecule and a free $OZn_4(HCO_2)_6$ cluster and found that the interaction with the cluster was about 70 meV/molecule, stronger than with the benzene molecule, 25–35 meV/molecule. Kuc *et al.*[20,21] reported that the highest MP2 energies on the $C_6H_4(COOH)_2$ and ZnO_4H_6 clusters were 35 and 50 meV/molecule, respectively.

Although both DFT and MP2 calculations indicate that the adsorption near the metal oxide core is larger than on the benzene ring, they differ in the magnitude of the physisorption energies: DFT yields energies of 100–160 meV/molecule on the oxide core and 70–90 meV/molecule on the benzene ring, while the MP2 method yields smaller energies of 50–70 and 25–35 meV/molecule on the oxide core and on the benzene ring, respectively. The MP2 results are more accurate, but they have been obtained using very small parts or clusters of the MOF-5 structure. However, these weak interactions are additive and the MP2 energies are missing the interactions with the other atoms. On the other hand, the present DFT calculations are less accurate, but they consider all the atoms.

The main adsorption regions that we have identified in the analysis of the PES are consistent with the adsorption sites obtained in the experimental study of Yildirim and Hartman.[12] These authors analyzed neutron powder-diffraction data with Rietveld and Fourier techniques and a model of the structure of MOF-5. They found that the most important adsorption site was the "cup site." This site corresponds to the deep potential well of region A (see Fig. 5). Further refinement yielded three other sites called ZnO_3, ZnO_2, and Hex by these authors. Sites ZnO_3 and ZnO_2 are very close to one another. These are located on region B, which we call the long trench. Finally, Hex site is our region C on the benzene ring of the BDC linker. They performed LDA calculations and obtained adsorption energies similar to those presented in this paper. However, our PES offers substantial additional insight, especially with respect to the shape of the adsorption regions. First, the highest adsorption energies occur in extended regions called A and B here rather

than at specific sites. Second, region B contains more sites than just the ZnO_3 and ZnO_2 sites. This is an extended region with the structure of a long trench. The areas of highest adsorption energies in regions A and B are connected forming an extended trench following the borders of some O-Zn-O-C-O-Zn hexagons, as can be seen in Fig. 5, with a barrier of about 30–50 meV/molecule between regions A and B. This long adsorption trench explains why some authors associated just one main physisorption site to the oxide core,[6] while other authors identified two main sites near that oxide core[13] and Yildirim and Hartman[12] identified three sites. Rosi *et al.*[6] identified two different adsorption sites in their inelastic neutron-scattering experiments and associated one to Zn and the other to the BDC linker. Two years later, Mueller and Ceder[13] performed DFT calculations and proposed a different explanation, namely, that both sites are near the metal oxide core and not near the BDC linker. All those discrepancies are now resolved by the present calculations.

The most important information that can be extracted from the PES is that the available adsorption areas, that is, the local minima in the PES, are the borders of some particular regions of the atomic framework of the MOF-5 structure. Those regions appear in the form of long trenches. Due to the hollow structure of the material, there are many of those adsorption trenches near the oxide core tetrahedra on the vertices of the cubes forming the structure of MOF-5 (see Fig. 1). To these regions one has to add adsorption sites at the BDC linkers. The very weak interaction between hydrogen molecules compared to the interaction with the MOF-5 surface indicates that the adsorbed population of one adsorption region does not affect adjacent regions. This explains the large hydrogen storage capacity of this material, MOF-5. The calculations show that having a hollow almost empty structure is not enough to get large hydrogen storage capacities because the PES displays, apart from the local minima and the adsorption trenches, wide "flatland" regions of near zero or positive interaction energies which cannot store hydrogen unless enough external pressure is applied.

IV. DISSOCIATIVE CHEMISORPTION

We have also studied the dissociative chemisorption of the hydrogen molecule on the MOF-5. Between the possible chemisorption sites, the oxygen atoms seem to be the most favorable ones, and we have selected the two oxygen atoms labeled O_A and O_B which are part of the O-Zn-O-C-O-Zn hexagon in Fig. 3. After adsorbing the two hydrogen atoms in those positions, as shown in Fig. 6, the structure of the system was optimized by relaxing the positions of the O_A, O_B, and H atoms. The chemisorption energy, measured with respect to two separated H atoms

$$E_{\text{chem}} = E(\text{MOF-5}) + 2E(\text{H}) - E(2\text{H} - \text{MOF-5}) \qquad (2)$$

is 2.66 eV (1.33 eV/H atom). The chemisorption of the two H atoms distorts substantially the host hexagon: the interatomic distances d_{C-O}, d_{O-O}, and d_{Zn-O} increase by 0.14, 0.07, and 0.05 Å, respectively, and the O-C-O angle decreases by 14.5°. On the other hand, if we notice that the experimental energy required to dissociate the free H_2 molecule in two H atoms is 4.75 eV, we find that the physisorbed H_2 molecule is more stable than the dissociated chemisorbed state by about 2 eV.

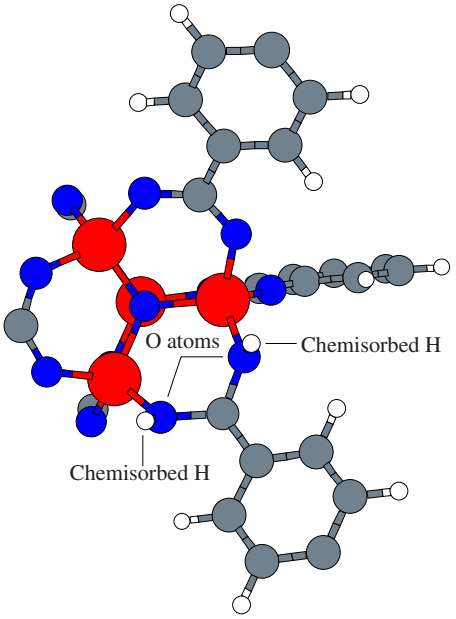

FIG. 6. (Color online) Dissociative chemisorption of a hydrogen molecule on the oxygen atoms O_A and O_B of the O_{core}-Zn_A-O_A-C-O_B-Zn_B hexagon. The H-H distance in the chemisorbed geometry is 2.93 Å.

Reaching the chemisorption state requires dissociating the H_2 molecule. The cost of 4.75 eV for dissociating the free molecule decreases a little for an adsorbed molecule, but still the dissociation barrier is large. We have estimated the dissociation barrier for the adsorbed hydrogen molecule by calculating the energy for a number of configurations along the dissociation path. In each configuration the distance between the two H atoms takes a fixed value, and the positions of the two hydrogen atoms and the two oxygen atoms are relaxed subject to that constraint. The calculations indicate an upper bound of 4 eV for the barrier. The dissociation barrier on MOF-5 is higher than on carbon nanotubes.[22–24]

V. CONCLUSIONS AND COMMENTS

We have performed extensive DFT calculations of the interaction of H_2 with the highly porous material MOF-5. The obtained potential-energy surface indicates that there are two main adsorption regions and that they are near the OZn_4 oxide cores at the corners of the MOF-5 structure. Those regions have the shape of long, wide, and deep trenches in different octants merging at a given OZn_4 corner. Those trenches are connected and passage of adsorbed molecules between the trenches requires a small activation energy of about 30–50 meV/molecule. Only a small portion of the trenches is near a Zn atom and, hence, the presence of transition-metal atoms is not the only explanation of the large hydrogen physisorption and storage capacities of MOF-5, as some authors suggested, but also the extended shape of those regions and their attractive potential. Our

opinion is that the main role of transition-metal atoms is that their chemical coordination allows to build open, porous, and stable structures (the MOFs) with a larger effective surface interacting with the hydrogen molecules compared to other materials.

The elongated shape of the adsorption regions also explains why some authors reported only one adsorption site associated to the Zn oxide core and others reported two or even three sites. These trenches contain the sites identified until now in experiments and calculations, but we stress that the adsorption regions are extended not just localized sites. The potential-energy surface indicates that there are also large flat regions in MOF-5 that cannot adsorb molecules because the interaction potential is near zero in those regions. Hence, in the search for good porous materials for hydrogen storage an optimal size of the pores is very important.[25,26] In a pore with a large volume, only the part of the volume in contact with the inner surface of the pore is effective in storing gas.

We have studied also the dissociative chemisorption of the hydrogen molecule. The chemisorption energy with respect to two separated H atoms is 2.66 eV (1.33 eV/H atom); but because it costs 4.75 eV to dissociate the molecule, the physisorbed H_2 molecule is more stable than the dissociated chemisorbed state by about 2 eV. Dissociating the adsorbed molecule costs less energy, but the barrier is still substantial.

ACKNOWLEDGMENTS

This work was supported by MEC of Spain (Grants No. MAT2004-23280-E and No. MAT2005-06544-C03-01), Junta de Castilla y León (Grants No. VA039A05, No. VA017A08, and No. GR23), and the University of Valladolid. I.C. acknowledges support from MEC-FSE through the Ramón y Cajal Program. J.A.A. acknowledges the hospitality and support of Donostia International Physics Center. We acknowledge the computer resources and assistance provided by the Altamira node at University of Cantabria of the Spanish Supercomputing Network (RES), where part of the calculations were done. We are also thankful for the help of A. Mañanes.

[1] http://www1.eere.energy.gov/hydrogenandfuelcells/pdfs/freedomcar_targets_explanations.pdf
[2] Multi-Year Research, Development and Demonstration Plan: Planned Program Activities for 2003–2010: Technical Plan, U. S. Department of Energy, http://www.eere.energy.gov/hydrogenandfuelcells/mypp/pdfs/storage.pdf
[3] A. Züttel, Mater. Today **6**, 24 (2003).
[4] S. Orimo, A. Züttel, L. Schlapbach, G. Majer, T. Fukunaga, and H. Fujii, J. Appl. Crystallogr. **356**, 716 (2003).
[5] L. Hailian, M. Eddaoudi, M. O'Keeffe, and O. M. Yaghi, Nature (London) **402**, 276 (1999).
[6] N. Rosi, J. Eckert, M. Eddaoudi, D. T. Vodak, J. Kim, M. O'Keeffe, and O. M. Yaghi, Science **300**, 1127 (2003).
[7] J. L. C. Rowsell, A. R. Millward, K. S. Park, and O. M. Yaghi, J. Am. Chem. Soc. **126**, 5666 (2004).
[8] A. G. Wong-Foy, A. J. Matzger, and O. M. Yaghi, J. Am. Chem. Soc. **128**, 3494 (2006).
[9] B. Panella, M. Hirscher, H. Pütter, and U. Müller, Adv. Funct. Mater. **16**, 520 (2006).
[10] H. K. Chae, D. Y. Siberio-Pérez, J. Kim, Y. Go, M. Eddaoudi, A. J. Matzger, M. O'Keeffe, and O. M. Yaghi, Nature (London) **427**, 523 (2004).
[11] T. Sagara, J. Klassen, and E. Ganz, J. Chem. Phys. **121**, 12543 (2004).
[12] T. Yildirim and M. R. Hartman, Phys. Rev. Lett. **95**, 215504 (2005).
[13] T. Mueller and G. Ceder, J. Phys. Chem. B **109**, 17974 (2005).
[14] A. Samanta, T. Furuta, and J. Li, J. Chem. Phys. **125**, 084714 (2006).
[15] F. M. Mulder, T. J. Dingemans, M. Wagemaker, and G. J. Kearley, Chem. Phys. **317**, 113 (2005).
[16] S. H. Vosko, L. Wilk, and M. Nusair, Can. J. Phys. **58**, 1200 (1980).
[17] http://dcwww.camp.dtu.dk/campos/Dacapo
[18] S. Bordiga, C. Lamberti, G. Ricchiardi, L. Regli, F. Bonino, A. Damin, K. P. Lillerud, M. Bjorgen, and A. Zecchina, Chem. Commun. (Cambridge) 2004, 2300 (2004).
[19] I. Cabria, M. J. López, and J. A. Alonso, J. Chem. Phys. **123**, 204721 (2005).
[20] A. Kuc, T. Heine, G. Seifert, and H. A. Duarte, Chem.-Eur. J. **14**, 6597 (2008).
[21] A. Kuc, T. Heine, G. Seifert, and H. A. Duarte, Theor. Chim. Acta **120**, 543 (2008).
[22] K. Tada, S. Furuya, and K. Watanabe, Phys. Rev. B **63**, 155405 (2001).
[23] J. S. Arellano, L. M. Molina, A. Rubio, M. J. López, and J. A. Alonso, J. Chem. Phys. **117**, 2281 (2002).
[24] G. Chen, X. G. Gong, and C. T. Chan, Phys. Rev. B **72**, 045444 (2005).
[25] I. Cabria, M. J. López, and J. A. Alonso, Carbon **45**, 2649 (2007).
[26] Figure 8 of the above reference contains two errors: the gravimetric capacities of Q. Wang and J. K. Johnson [J. Chem. Phys. **110**, 577 (1999)] at 77 K should be about 3 and 7 wt % for slitpores of 6 and 9 Å of width, respectively, instead of 0.2 and 0.5 wt %.